Version of: August 13, 2003

What is the role of the kink instability in solar coronal eruptions?

Robert J. Leamon, Richard C. Canfield and Zachary Blehm

Montana State University, Department of Physics, Bozeman, MT 59717

Alexei A. Pevtsov

National Solar Observatory/ Sacramento Peak, Sunspot, NM 88349

ABSTRACT

We report the results of two simple studies which seek observational evidence that solar coronal loops are unstable to the MHD kink instability above a certain critical value of the total twist. First, we have used Yohkoh SXT image sequences to measure the shapes of 191 X-ray sigmoids and to determine the histories of eruption (evidenced by cusp and arcade signatures) of their associated active regions. We find that the distribution of sigmoid shapes is quite narrow and the frequency of eruption does not depend significantly on shape. Second, we have used Mees Solar Observatory vector magnetograms to estimate the large-scale total twist of active regions in which flare-related signatures of eruption are observed. We find no evidence of eruption for values of large-scale total twist remotely approaching the threshold for the kink instability.

Subject headings: Sun: corona — Sun: magnetic fields — Sun: X-rays, gamma rays — Sun: coronal mass ejections

1. Introduction

As viewed by the *Yohkoh* Soft X-Ray Telescope (SXT: Tsuneta et al. (1991)), coronal active regions comprise discrete bright loops that outline magnetic field lines. These loops often singly or collectively form sinuous S or 2 shapes, termed *sigmoids* by Rust & Kumar (1994). They found transient X-ray brightenings that typically evolved from bright, sharp-edged sigmoidal features into either an arcade of loops or a diffuse cloud. The latter

phenomenon—related to long-duration events, or LDEs—was discovered in the Skylab era of X-ray imaging (Kahler 1977, 1992; Webb 2000), but its relevance has come to be appreciated more broadly since Sterling & Hudson (1997) and Hudson et al. (1998) combined *Yohkoh* SXT images with those of the LASCO coronagraph (Brueckner et al. 1995), revealing what they call the "sigmoid → arcade" signature of eruption. This pattern occurred repeatedly in a study of low-coronal counterparts of halo CMEs (Hudson et al. 1998). The utility of the "sigmoid → arcade" phenomenon became clear when Canfield et al. (1999) demonstrated that active regions containing X-ray sigmoids are more likely to erupt. Subsequent work (*e.g.*, Glover et al. 2001) clarified this finding, drawing a distinction between single loops and patterns formed by collections of loops. Importantly, Leamon et al. (2002) showed that when active region sigmoids do erupt, they tend to produce at least moderate (and often major) geomagnetic storms.

As the result of MHD research dating from the 1950s, it is known that the total (end-to-end) twist in a given magnetic loop is a major factor in its MHD stability. A cylindrical force-free magnetic field is stable to the helical kink instability (in which 2π of twist about the tube axis is converted into writhe of the tube axis – see Berger (1999) for a discussion of twist and writhe in the framework of magnetic helicity) only for total twist below a critical value $T_c \sim 2\pi$ (Priest 1984), i.e., about one turn. For more realistic models of solar loops, T_c exceeds 2π by factors of order unity that depend on radial profiles of currents and fields, boundary conditions, and loop geometry. For example, Mikic et al. (1990) found $T_c \sim 4.8\pi$ on the axis of an initially purely axial loop created by twisting its footpoints. Moreover, the presence of an overlying arcade field can have a stabilizing effect that makes the kink instability moot, preventing the escape of the twisted loop (Antiochos et al. 1999; Roussev et al. 2003) in spite of kinking. For purposes of discussion, we simply assume that the relevant critical value is $T_c \sim 2\pi$.

Previous observers have sought evidence of the kink instability in coronal data. Rust & Kumar (1996) compared the shape of 49 transient, bright sigmoid structures to the geometry of a helically kinked flux rope. They *assumed* this rope to have 2π of writhe over its length, and showed that the distribution of sigmoids as a function of aspect ratio falls off abruptly below the threshold for the $m = 1$ kink mode in this model. From this observation they inferred that kinking is the cause of eruption. Similarly, observations of prominences were described by Vršnak et al. (1991) in terms of the pitch angle of the helical structure. They found that no eruptive prominence had a total twist $< 2\pi$ (*i.e.*, less than one complete turn). Conversely, all prominences that had a total twist $\geq 2.5\pi$ (*i.e.*, one-and-a-quarter turns) erupted.

Unfortunately, many questions of interpretation arise when one tries to explain coronal

structures in terms of specific magnetic field topologies. For example, do sigmoids outline twisted field lines within regions that can be approximated by linear force-free fields in a bipolar active region (Pevtsov et al. 1997)? This interpretation is possible but not compelling, since field lines with both forward and backward-S shapes are present in such regions. Do sigmoids outline those particular field lines along which the largest currents flow (Magara & Longcope 2001)? The extremely low resistivity of the corona makes this explanation only marginally more plausible than the simple linear force-free model. Do they outline helically kinked flux tubes, assumed to possess 2π total writhe (Rust & Kumar 1996)? This explanation does not give the correct hemispheric rule for the shape of sigmoids. Kinking of an unwrithed tube whose initial twist (*e.g.*, left-handed in the Northern hemisphere) follows the well-known hemispheric helicity rule (Seehafer 1990; Pevtsov et al. 1995) necessarily produces a flux tube whose writhe is left-handed in the Northern hemisphere, by helicity conservation. Figure 2 of Longcope et al. (1998) shows that 2π left-handed writhe projects as an S shape there, rather than the S shape that is known to predominate (*e.g.*, Rust & Kumar 1996; Pevtsov et al. 2001). (This assumes that the field lines of the active region bulge up into the corona from below the photosphere; if they bulge down, they project as an S, but do not extend into the corona.) Finally, do sigmoids not outline field lines at all, but rather current sheets along the sinuous separatrix surfaces between a twisted toroidal flux tube and its surroundings (Titov & Démoulin 1999), which may be in the process of kinking (Fan & Gibson 2003)? This model is appealing in many respects, including its consistency with both the hemispheric helicity (twist) rule and the hemispheric dependence of sigmoid shapes (as shown by Fan & Gibson (2003)). However, the long lifetimes (days) of sigmoids (Pevtsov 2002) rule out the dynamic Fan & Gibson (2003) explanation for all but the transient bright sigmoids seen in the sigmoid-to-arcade phenomenon (Sterling & Hudson 1997; Hudson et al. 1998) at the time of eruptive flares, which attracted the attention of Rust & Kumar (1996).

Our hypothesis in this paper is that twisted coronal loops are unstable to the MHD kink mode only if their total twist exceeds a critical value, which in any case is not less than $T_c \sim 2\pi$. Athough we have carried out an observational study of the shapes of sigmoids, the uncertainties of interpretation reviewed above prevent us from relating them to the twist of their magnetic fields in a quantitative manner. Hence in Section 2 we simply describe our parameterization of the shapes of sigmoids, the distribution of the shape parameter, and the relationship of shape to frequency of eruption in our database. On the other hand, we can make an objective and quantitative study using vector magnetograms. In Section 3 we use this approach to determine the twist of the magnetic fields of active regions in the same manner that has been used to establish the hemispheric helicity rule (*e.g.*, Pevtsov et al. 1995; Pevtsov et al. 2001). We relate and interpret the results of these two approaches in Section 4, leading to the conclusion that our results are inconsistent with the kink instability

as the cause of solar eruptions.

2. Sigmoid Shapes

The coronal magnetic field $\mathbf{B}$ can be described to a good approximation as force-free, i.e., $\nabla \times \mathbf{B} = \alpha \mathbf{B}$ (Priest 1984). To parameterize the shape of sigmoids we follow Pevtsov et al. (1997), who used a two-dimensional linear force-free field solution for which

$$\alpha = \left(\frac{\pi}{L}\right) \cdot \sin\gamma. \tag{1}$$

Here L is the separation between endpoints of a loop and γ is the shear angle at which the central field line crosses the line joining its endpoints.

Equation (1) is only a two-dimensional solution, and the ambiguities reviewed in Section 1 cannot be ignored. Nevertheless, L and $\sin\gamma$ are physically motivated parameters, at least in two dimensions. Using an interactive image analysis tool to analyze the SXT images such as the one in Figure 1, we determined the values of L and γ for 191 coronal sigmoids observed between October 1991 and October 2000 (ARs 6871–9201). The distribution of $\sin\gamma$ values for the sigmoids in our dataset is shown in the upper panel of Figure 2. The most important feature of this histogram is that its width is not significantly different from what we would expect from the $\langle\Delta\gamma\rangle = 6^\circ$ uncertainty of measurement of γ. The corresponding distribution of L values is shown in the lower panel of Figure 2. The average shear angle $\langle\gamma\rangle = 32^\circ$ and the average length $\langle L\rangle = 160$ Mm. Independent estimates typically differed by $\langle\Delta\gamma\rangle = 6^\circ$ and $\langle\Delta L\rangle = 1$ Mm.

We do not attempt to infer a quantitative value of total twist from the average value of $\sin\gamma \sim 1/2$ at the peak of the distribution, for the reasons given in the preceding paragraph. The fact that the difference between the corrected and uncorrected histograms is so minor reflects that fact that sigmoids are not visible far from disk center. In our dataset their average angular distance from Sun center is only $24^\circ \pm 9.5^\circ$.

From the SXT images we have determined the histories of eruption of all regions for which we have L and γ values, using cusps and arcades as proxies for eruption (Sterling & Hudson 1997; Hudson et al. 1998; Canfield et al. 1999). From these histories we have determined the frequency of eruption per disk transit, taking into account the fraction for which a given region was present on the disk. The relationship between frequency of eruption and $\sin\gamma$ is shown in Figure 3. The fact that the one-σ error band brackets the null hypothesis (zero slope) confirms the visual impression that there is no relationship between frequency of eruption and sigmoid shape, perhaps because there is little or no real variation of shape,

which some might take as support for the argument that sigmoids outline separators, not field lines. Finally, Figure 3 also shows that not all sigmoids erupt during a disk transit, consistent with the results of Canfield et al. (1999).

3. Vector Magnetograms

In order to make a quantitative measurement of twist we turn to vector magnetograms, which have been used extensively to measure the twist of active region magnetic fields (Seehafer 1990; Pevtsov et al. 1994; Longcope et al. 1998). For many active regions, spanning October 1991 to December 1998 (ARs 6891–8410), we have both X-ray image sequences from the Yohkoh SXT and photospheric vector magnetograms from the Haleakala Stokes Polarimeter (Mickey 1985).

In order to have a single number with which to quantify the twist of the photospheric magnetic fields of an active region as a whole, Pevtsov et al. (1995) introduced $\alpha_{\rm best}$, the value of α for a linear force-free field that gives the best least-squares fit to the observed horizontal field in a vector magnetogram, constrained by the observed line of sight field. Leka (1999) found that this measure is quantitatively robust when proper attention is paid to noise. Longcope et al. (1998) showed that $\alpha_{\rm best}$ is related to the local twist of a simple flux tube q (radians per unit length) by $\alpha_{\rm best} = 2q$, where the total twist T is simply an integral of the local twist $T = \oint q dl$. Pevtsov et al. (2003) have demonstrated that within about a day after emergence, twist contained in a coronal flux system saturates to that in the associated flux tubes threading the photosphere at its footpoints. Time lags for twist to build up after flux tube emergence into the corona are therefore expected to play only a minor role in our database.

As above, we tally eruptive events identified by the presence of a cusp or arcade in the SXT data. However, to focus our attention on larger events, which are more likely to be geophysically interesting, we also require a flare (reported in Solar Geophysical Data) of a certain duration (beginning to end) in the active region of interest whose peak X-ray intensity occurs in the one-hour period prior to the time recorded for the eruptive event. To enable the determination of the twist of the active region magnetic field as a whole, we require that there be an HSP magnetogram of the region in which the eruption signature was observed within 24 hours of the time of eruption, since Pevtsov et al. (1994) found the characteristic evolutionary time of α patterns to be about 22 hours. This combination of requirements greatly reduces the number of events in our database, but the vector magnetograms allow us to quantify objectively both the separation L of the flux-weighted polarity centroids and $\alpha_{\rm best}$. The coronal field line length is then $\pi L/2$. Figure 4 shows a histogram of the 25 flare-associated

eruptive events with total twist measured by vector magnetograms $T = (\pi/4)\alpha_{\rm best} L$, and calls attention to the three longest-duration events (one just over one hour, two over two hours). Of the 25 events (but not the latter three), 5 show sigmoids in the course of eruption, and 10 others show them in the active regions of their occurrence at other times. Two properties are noteworthy. First, the distribution of T values in Figure 4 is broad, extending from the origin to slightly over 2π radians, not peaked at a given value. Second, many eruptions occur for total twists far less than 2π radians, and no eruptions occur for values remotely approaching the critical twist $T_c \sim 2\pi$ associated with the kink instability in the most simplistic models.

4. Discussion

The basic conclusion of this work is that the kink instability does not explain the eruptions of solar active regions, when α and L are inferred directly from vector magnetograms, as we have done. If the kink instability were the proper explanation for eruptions, the twist of regions that were in the process of eruption would be at or above the critical twist for the MHD kink instability in a simple cylindrical flux tube $T_c \sim 2\pi$. Figure 4 shows that the total twist of active regions in our dataset that exhibit flare-associated cusp/arcade signatures of eruptions in the SXT data is never more than about $2\pi/3$, and as often as not, is less than $2\pi/6$, much less than the value $T_c \sim 2\pi$ that is already a very conservative threshold for the kink instability.

How strong is the evidence for the narrow range of shapes of sigmoids in Figure 2? Many of these sigmoids in our database are transient, in the process of eruption. This observation of a limited range of shapes of such transient sigmoids is not new; Rust & Kumar (1996) also noted it. They *assumed* that this peak corresponded to a $m = 1$ helically kinked flux rope with 2π total coronal writhe, which in their notation is $kR = .581$. This aspect ratio corresponds to $\gamma = 30.16°$; we infer from their Figure 2 an average value of $kR = .855$, which corresponds to $\gamma = 40.5°$. Our measured average of 32° is close to the former, but significantly different from the latter. The uncertainty of our individual values is ±6°, but the average is defined to better than one degree. The less than perfect agreement of average values notwithstanding, both studies find that the distribution of sigmoid shapes is strongly peaked.

However, we have ruled out the Rust & Kumar (1996) interpretation because of its conflict with the hemispheric twist rule and helicity conservation (Section 1). What, then, is the proper explanation? The narrow range of $\sin\gamma$ values, in particular, suggests the onset of some instability at certain typical geometric parameters that show little intrinsic variability, for whatever reason. Is it simply that the sigmoids outline current sheets at separatrix

surfaces, as proposed by Titov & Démoulin (1999), which are formed during the kinking process (Fan & Gibson 2003)? The latter explanation circumvents the hemispheric twist rule conflict, but it is inconsistent with our total twist estimates. One obvious possibility, considering the results above, would seem to be that the eruption is associated with a subsystem of the active region that has a local twist much greater than $\alpha_{\rm best}$. Since it is known that patterns of $\alpha(x, y)$ exist in many active regions (Pevtsov et al. 1994), and the peak amplitude of $\alpha(x, y)$ can exceed that of $\alpha_{\rm best}$ by an order of magnitude, such a possibility cannot be ruled out. However, the highly non-local nature of the corona makes it hard to believe that the proper explanation does not lie in large-scale structure such as that measured by $\alpha_{\rm best}$. It is known that the largest-scale ($m = 1$) mode in highly symmetric systems is the least stable, and it is the twist of the larger-scale active region fields that is measured by $\alpha_{\rm best}$.

Yohkoh is a mission of ISAS in Japan; the SXT instrument is a collaboration of the University of Tokyo, the National Astronomical Observatory of Japan, and the Lockheed Martin Solar and Astrophysics Laboratory. The National Solar Observatory (NSO) is operated by the Association of Universities for Research in Astronomy (AURA, Inc.) under cooperative agreement with the National Science Foundation (NSF).

Funding for this work was provided by AFOSR under grant F49620-00-1-0128 and NASA under grant NAG5-11873.

REFERENCES

Antiochos, S. K., DeVore, C. R., & Klimchuk, J. A. 1999, ApJ, 510, 485

Berger, M. A. 1999, in Geophys. Monogr. Ser., Vol. 111, Magnetic Helicity in Space and Laboratory Plasmas, ed. M. R. Brown, R. C. Canfield, & A. A. Pevtsov (Washington, D.C.: AGU), 1–10

Brueckner, G. E., Howard, R. A., Koomen, M. J., Korendyke, C. M., Michels, D. J., Moses, J. D., Socker, D. G., Dere, K. P., Lamy, P. L., Llebaria, A., Bout, M. V., Schwenn, R., Simnett, G. M., Bedford, D. K., & Eyles, C. J. 1995, Solar Phys., 162, 357

Canfield, R. C., Hudson, H. S., & McKenzie, D. E. 1999, Geophys. Res. Lett., 26, 627

Fan, Y. & Gibson, S. E. 2003, ApJ, 589, L105

Glover, A., Harra, L. K., Matthews, S. A., Hori, K., & Culhane, J. 2001, A&A, 378, 239

Hudson, H. S., Lemen, J. R., St. Cyr, O. C., Sterling, A. C., & Webb, D. F. 1998, Geophys. Res. Lett., **25**, 2481

Kahler, S. 1977, ApJ, 214, 891

Kahler, S. W. 1992, ARA&A, 30, 113

Leamon, R. J., Canfield, R. C., & Pevtsov, A. A. 2002, J. Geophys. Res., 107, 1234

Leka, K. D. 1999, Solar Phys., 188, 21

Longcope, D. W., Fisher, G. H., & Pevtsov, A. A. 1998, ApJ, 507, 417

Magara, T. & Longcope, D. W. 2001, ApJ, 559, L55

Mickey, D. L. 1985, Solar Phys., 97, 223

Mikic, Z., Schnack, D. D., & van Hoven, G. 1990, ApJ, 361, 690

Pevtsov, A. A. 2002, in COSPAR Colloquia Series, Vol. 13, Multi-Wavelength Observations of Coronal Structure and Dynamics, ed. P. C. H. Martens & D. P. Cauffman (Amsterdam: Pergamon), 125

Pevtsov, A. A., Canfield, R. C., & Latushko, S. M. 2001, ApJ, 549, L261

Pevtsov, A. A., Canfield, R. C., & McClymont, A. N. 1997, ApJ, 481, 973

Pevtsov, A. A., Canfield, R. C., & Metcalf, T. R. 1994, ApJ, 425, L117

—. 1995, ApJ, 440, L109

Pevtsov, A. A., Maleev, V. M., & Longcope, D. W. 1998, ApJ, 593, 1217

Priest, E. R. 1984, Solar Magneto-Hydrodynamics, Geophysics and Astrophysics Monographs (Dordrecht: Reidel)

Roussev, I. I., Forbes, T. G., Gombosi, T. I., Sokolov, I. V., DeZeeuw, D. L., & Birn, J. 2003, ApJ, 588, L45

Rust, D. M. & Kumar, A. 1994, Solar Phys., 155, 69

—. 1996, ApJ, 464, L199

Seehafer, N. 1990, Solar Phys., 125, 219

Sterling, A. C. & Hudson, H. S. 1997, ApJ, 491, L55

Titov, V. S. & Démoulin, P. 1999, A&A, 351, 707

Tsuneta, S., Acton, L., Bruner, M., Lemen, J., Brown, W., Caravalho, R., Catura, R., Freeland, S., Jurcevich, B., & Owens, J. 1991, Solar Phys., 136, 37

Vršnak, B., Ruždjak, V., & Rompolt, B. 1991, Solar Phys., 136, 151

Webb, D. F. 2000, IEEE Trans. Plasma Sci., 28, 1795

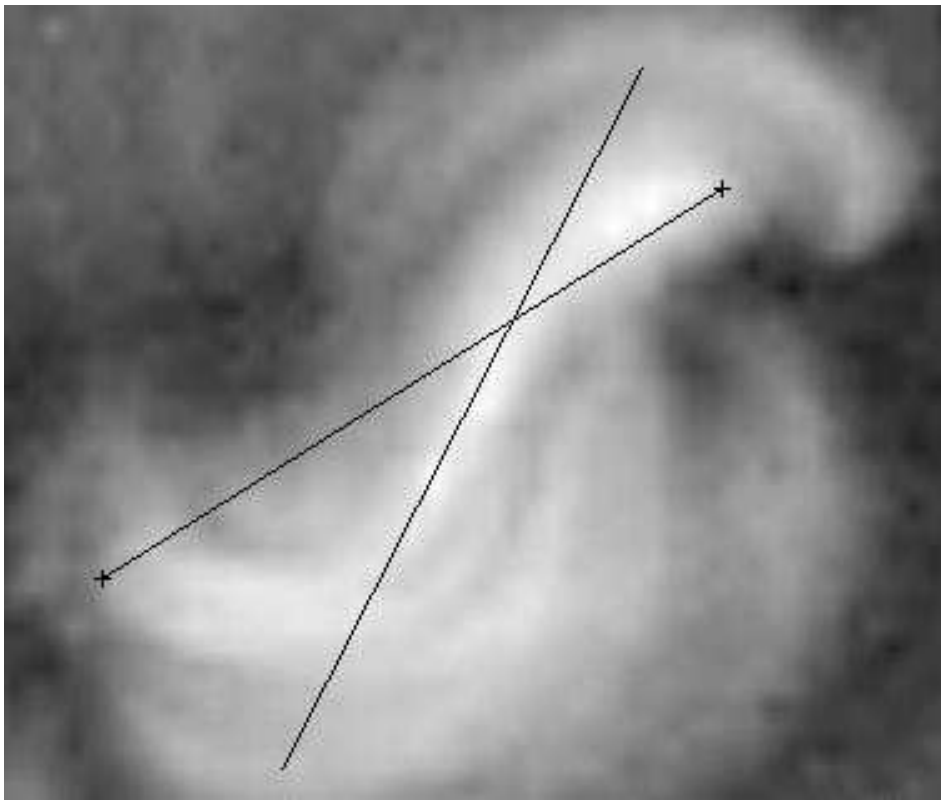

Fig. 1.— Yohkoh SXT image (11 January 1993 08:39:44) of a sigmoid, showing lines (the sigmoid "skeleton") used in the interactive image analysis tool to determine the dimension L and shear angle γ. The length L is the distance between the apparent ends of the brightest loops of the sigmoid, marked with + symbols. The shear angle γ is the acute angle between this line and a tangent to the central loops of the sigmoid. For this example $L = 257$ Mm and $\gamma = 31°$, both rather typical values.

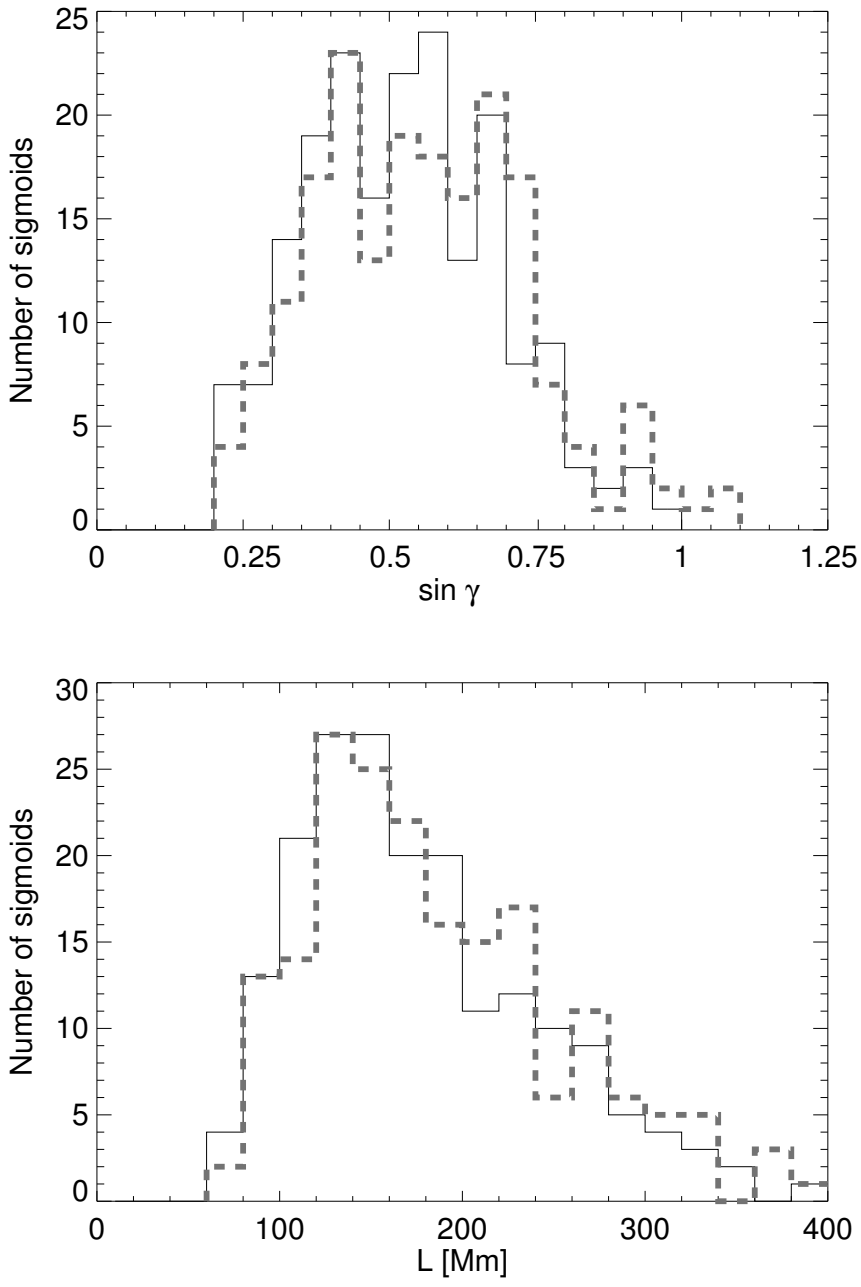

Fig. 2.— The distributions of $\sin\gamma$ and L values in the 191 sigmoids of our dataset. Solid lines: as measured. Dashed grey lines: corrected for projection effects.

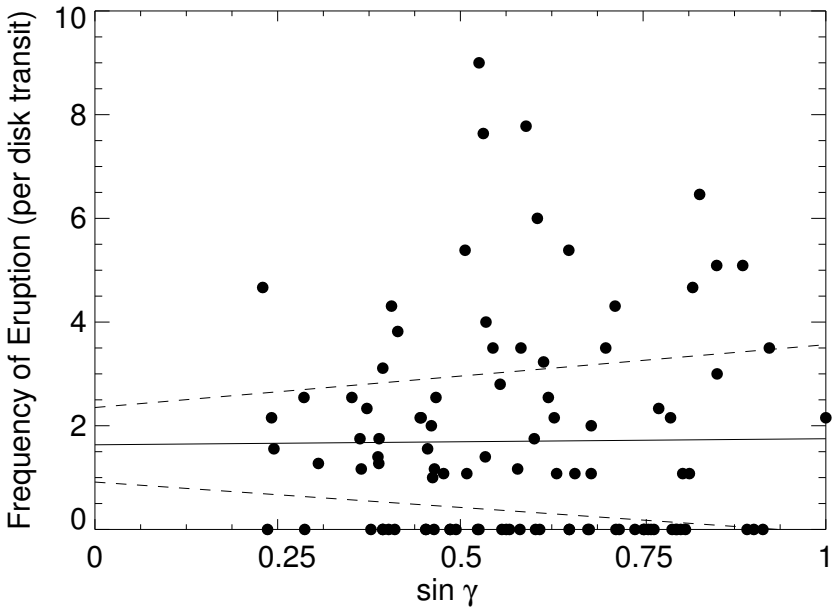

Fig. 3.— The number of eruptions per active region, scaled per solar disk transit, as a function of $\sin\gamma$ determined from sigmoid "skeletons." The solid line is the best linear fit; the dashed lines show the range associated with the 1σ error bars in the fitting parameters.

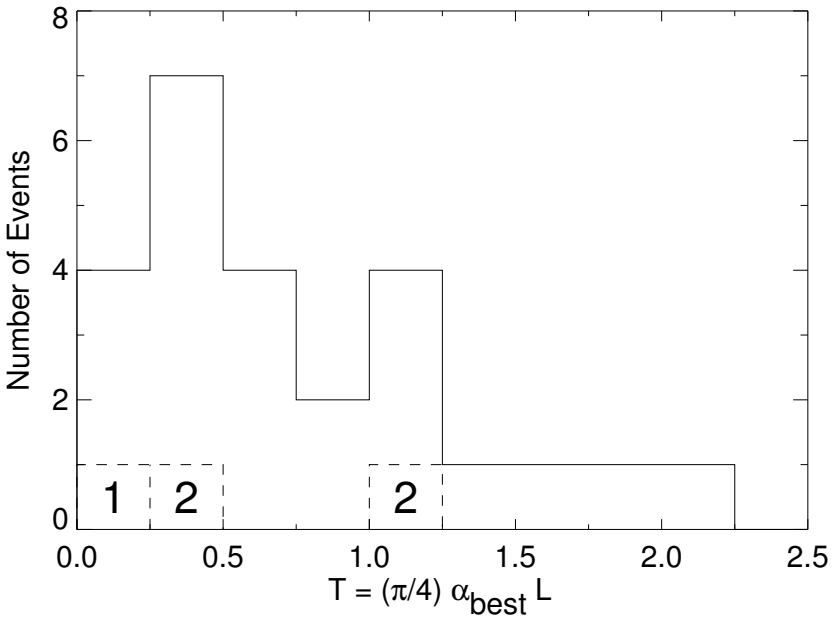

Fig. 4.— Histogram of 25 flare-associated eruptive events for which the total coronal twist T has been determined from vector magnetograms. The three numbered events (dashed lines) are those with longest flare durations, exceeding 1, 2, and 2 hours respectively.